12-2012

High-order-harmonic-generation spectroscopy with an elliptically polarized laser field

M. V. Frolov
Voronezh State University, Russia, frolov@phys.vsu.ru

N. L. Manakov
Voronezh State University, Russia, manakov@phys.vsu.ru

T. S. Sarantseva
Voronezh State University, Russia, sarantseva@phys.vsu.ru

Anthony F. Starace
University of Nebraska-Lincoln, astarace1@unl.edu

High-order-harmonic-generation spectroscopy with an elliptically polarized laser field

M. V. Frolov,[1] N. L. Manakov,[1] T. S. Sarantseva,[1] and Anthony F. Starace[2]
[1]*Department of Physics, Voronezh State University, Voronezh 394006, Russia*
[2]*Department of Physics and Astronomy, The University of Nebraska, Lincoln, Nebraska 68588-0299, USA*
(Received 28 September 2012; published 13 December 2012)

Analytic formulas describing high-order-harmonic generation (HHG) by atoms in an intense laser field with small ellipticity are obtained quantum mechanically in the tunneling limit. The results show that factorization of the HHG yield in terms of an electron wave packet and the photorecombination cross section (PRCS) is valid only for s states of a bound atomic electron, whereas the HHG yield for p states involves two different atomic parameters. For the latter case, elliptic HHG spectroscopy enables one to retrieve both the energy and angular dependence of the PRCS of the target atom, as we illustrate for the case of HHG by Xe in a midinfrared laser field.

DOI: 10.1103/PhysRevA.86.063406 PACS number(s): 32.80.Rm, 42.65.Re, 34.50.Rk, 42.50.Hz

I. INTRODUCTION

The ellipticity of a laser field provides an additional control parameter for laser-atom interactions and introduces some special features in nonlinear photoprocesses. For high-order-harmonic generation (HHG), these include the intensity-dependent difference between the polarizations of harmonics and the laser field [1–6], as well as more subtle features, such as elliptic dichroism [4] and the offset angle between the major axis of polarization of a harmonic and that of the laser field [7]. These latter two effects originate from an unusual kind of interference [4] (i.e., that between the real and imaginary parts of the HHG amplitude), which is very sensitive to the atomic dynamics, thereby providing an effective tool for testing the accuracy of different laser-atom interaction models.

Study of HHG in an elliptically polarized field began in 1980 with a perturbative (in the laser intensity) analysis [1] that predicted a power decrease of the HHG yield with increasing ellipticity that was confirmed experimentally [8,9] in the multiphoton regime, $\gamma > 1$, where γ is the Keldysh parameter [10]. In the strong field (tunneling) regime, $\gamma < 1$, experiments [8,11,12] observed a much steeper decrease, shown as Gaussian in a recent experiment [13]. In this regime, HHG in an elliptically polarized field has been treated theoretically using the strong field approximation (SFA) [2,3] to analyze the HHG yield [5] and the harmonic polarizations [2,3,6].

At present there is growing interest in the dependence of HHG on the driving laser ellipticity stimulated by the development of new methods for producing attosecond pulses (cf., e.g., Ref. [14]), as well as by applications to HHG-based spectroscopy of atoms and molecules. The ellipticity dependence of the HHG yield has been studied in Refs. [13,15–17]. A new technique for generation of elliptically-polarized attosecond pulses was proposed in Ref. [18] by means of HHG from atomic states having nonzero angular momentum. The polarization parameters of harmonics have been studied in Refs. [19,20] by employing a beyond-SFA analytical model [21] in combination with numerical solution of the time-dependent Schrödinger equation (TDSE). Measurements of the polarization vector of harmonics generated by Ar in an elliptically polarized field have been performed in Ref. [22]. The ellipticity-induced broadening of the Cooper minimum in the photorecombination cross section (PRCS) was observed in HHG spectra for Ar in Ref. [23].

HHG spectroscopy is based on the idea that the HHG yield can be factorized in terms of laser [the electron wave packet (EWP)] and atomic (the PRCS) parameters, thus allowing one to retrieve the field-free PRCS (or, equivalently, the photoionization cross section related to the PRCS according to the principle of detailed balance) from measured HHG spectra (cf., e.g., Ref. [24]). For a linearly polarized field, this factorization was proposed phenomenologically, based on numerical solutions of the TDSE [25]. It has now been justified theoretically for both a monochromatic field [26] and for short laser pulses [27]. However, questions on the possibility of factorization of the HHG yield for an elliptically polarized field, as well as on the information on field-free atomic dynamics that can be retrieved from measurements of HHG in an elliptically polarized field, remain unexplored. Concerning the latter question, we note that for linear polarization HHG measurements allow retrieval of only the energy dependence of the PRCS for zero angle between the polarization axis and the recombining electron momentum, while the angular dependence of the PRCS (described by the asymmetry parameter β [28]) remains unknown.

In this paper we report an analytic description of HHG by an intense laser field with small ellipticity that is valid for the plateau cutoff region of the HHG spectrum. A main goal is to show the strict difference between HHG yields for atoms having valence electrons with zero or nonzero orbital angular momentum, l. Our key result (53) parametrizing the HHG amplitude shows that while factorization of the HHG yield is possible for an s state, it is impossible for p states since the yield involves two parameters describing the field-free atomic dynamics. As we show, measurement of the HHG yield for a p state allows one, in contrast to experiments with linear polarization, to retrieve both the energy and the angular dependence of the PRCS.

This paper is organized as follows. In Sec. II we discuss briefly the extension of time-dependent effective range (TDER) theory [29], used previously by us to describe HHG in a linearly polarized field, to the case of HHG for a nonzero driving laser ellipticity. In particular, we provide a quasiclassical TDER result for the HHG amplitude for the case

of nonzero ellipticity in the low-frequency limit, and discuss its relation to both SFA results and TDER results for the case of linear polarization. In Sec. III we utilize the results of Sec. II for the plateau cutoff region of the HHG spectrum, discussing first the general case of nonzero ellipticity (Sec. III A) and providing then analytic expressions for the case of a small ellipticity (Sec. III B). In Sec. III C we present the key result of this paper: the factorized matrix form of the HHG amplitude. In Sec. IV A we discuss the factorized HHG rate for the case of an initial s state, while in Sec. IV B we consider the case of an initial p state. In the latter case we show how the angular dependence of the PRCS can be retrieved from HHG polarization measurements. Finally, we conclude in Sec. V.

II. QUASICLASSICAL TDER RESULTS FOR THE HHG RATE IN AN ELLIPTICALLY POLARIZED LASER FIELD

We consider the HHG process for a monochromatic, elliptically polarized laser field with electric vector

$$\mathbf{F}(t) = \mathcal{F}(\hat{\mathbf{x}}\cos\omega t + \hat{\mathbf{y}}\eta\sin\omega t), \quad \mathcal{F} = F/\sqrt{1+\eta^2}, \quad (1)$$

where F, ω, and η are the field amplitude, frequency, and ellipticity. Our atomic model is that of an electron in a short-range potential $U(r)$ supporting a single bound state, $\psi_{\kappa lm}(\mathbf{r}) = \varphi_{\kappa l}(r)Y_{l,m}(\hat{\mathbf{r}})$, with energy $E_0 = -\hbar^2\kappa^2/(2m)$ and angular momentum l. [In this paper we consider only cases of s ($l=0$) and p ($l=1$) states.] This model permits an exact solution for the HHG problem within the framework of TDER theory [29], which combines the quasistationary quasienergy state (QQES) approach [30] (for an exact account of the electron's interaction with a strong laser field) with effective range theory [31] (for a nonperturbative account of the electron's interaction with a potential $U(r)$ in terms of the scattering phase in the l-wave channel, $\delta_l(E)$, which is parametrized in terms of two fundamental parameters of effective range theory: the scattering length, a_l, and the effective range, r_l [31]). This approach for describing HHG by a linearly polarized field has been presented in detail in Ref. [32]. We extend it here to the case of nonzero ellipticity.

Since the angular momentum projection m [where we assume the quantization axis z is directed along the propagation axis of the field $\mathbf{F}(t)$] is not conserved in an elliptically polarized field, degenerate field-free states $\psi_{\kappa lm}(\mathbf{r})$ with different m are mixed by the field and evolve to the $(2l+1)$ different QQESs $\Phi_{\epsilon_q lq}(\mathbf{r},t)$ with complex quasienergies $\epsilon_q = E_0 + \Delta\epsilon_q$ enumerated by the index q (for a p state, $q=-1,0,1$) [29]. The exact TDER rate, $\mathcal{R}_l(N;\mathbf{e}')$, for coherent emission of the Nth harmonic (with energy $E_\Omega = N\hbar\omega$ and polarization vector $\mathbf{e}'$) from the initial state with angular momentum l is given by [33]

$$\mathcal{R}_l(N;\mathbf{e}') = \frac{(N\omega)^3}{2\pi\hbar c^3}\frac{1}{2l+1}\sum_{q=-l}^{l}|\mathcal{A}_{l,q}(N;\mathbf{e}')|^2, \quad (2)$$

where $\mathcal{A}_{l,q}(N;\mathbf{e}')$ is the HHG amplitude,

$$\mathcal{A}_{l,q}(N;\mathbf{e}') = (\mathbf{e}'^{*}\cdot\mathbf{d}_{l,q}), \quad (3)$$

and the dipole moment $\mathbf{d}_{l,q}$ is the Nth Fourier coefficient of the time-dependent dual dipole moment $\tilde{\mathbf{d}}_{l,q}(t)$ calculated with the QQES wave function $\Phi_{\epsilon_q lq}(\mathbf{r},t)$ (cf. Sec. II C of Ref. [33]). As in the case of linear polarization [32], the exact TDER amplitude $\mathcal{A}_{l,q}(N;\mathbf{e}')$ can be presented as a sum of integrals involving Bessel functions.

An analytic treatment of HHG is simplified in the quasiclassical (low-frequency) approximation [which is valid in the tunneling regime, $\gamma = \hbar\omega\kappa/(|e|F) \ll 1$]. In this approximation, we can approximate the quasienergy ϵ_q by E_0, while the QQES wave functions $\Phi_{\epsilon_q lq}(\mathbf{r},t)$ for initial s ($l=0$) or p ($l=1$) states reduce to superpositions of initially degenerate bound states $\psi_{\kappa lm}(\mathbf{r}) = \varphi_{\kappa l}(r)Y_{l,m}(\hat{\mathbf{r}})$ that follow from the exact TDER wave function in an elliptically polarized field [29] in the limit that the field $\mathbf{F}(t)$ is turned off,

$$\begin{aligned}&\varphi_{\kappa lq}(\mathbf{r}) = \varphi_{\kappa l}(r)f_{l,q}(\hat{\mathbf{r}}), \quad f_{l,0}(\hat{\mathbf{r}}) = Y_{l,0}(\hat{\mathbf{r}}),\\ &f_{1,\pm1}(\hat{\mathbf{r}}) = [Y_{1,1}(\hat{\mathbf{r}}) \pm Y_{1,-1}(\hat{\mathbf{r}})]/\sqrt{2},\end{aligned} \quad (4)$$

where $\varphi_{\kappa l}(r) = -i^l\kappa^{3/2}C_{\kappa l}h_l^{(1)}(i\kappa r)$ is the radial wave function within TDER theory, $h_l^{(1)}(x)$ is the spherical Hankel function of the first kind, and $C_{\kappa l}$ is the asymptotic coefficient. ($C_{\kappa l}$ and κ are parameters of the problem; they can be expressed in terms of a_l and r_l [29].) Note that the superpositions $f_{1,q}(\hat{\mathbf{r}})$ define states oriented along the three coordinate axes: x ($q=-1$), y ($q=1$), and z ($q=0$).

In the quasiclassical approximation, the exact TDER result for the dipole moment $\mathbf{d}_{l,q}$ in Eq. (3) reduces to a one-dimensional integral similar to that for a linearly polarized field $\mathbf{F}(t)$ [34],

$$\begin{aligned}\mathbf{d}_{l,q} = e\frac{2C_{\kappa,l}}{iT(\kappa a)^{3/2}}\int_{T/2}^{T} f_{l,q}[\hat{\mathbf{K}}_i(t)]\left(\frac{\mathbf{F}(t_i)}{F_0}\cdot\frac{\mathbf{K}_i(t)}{\hbar\kappa}\right)^{-1/2}\\ \times\frac{e^{-i[S(t,t_i)-Et+E_0t_i]/\hbar}}{[v_{\rm at}(t-t_i)]^{3/2}}\langle\varphi_{\kappa lq}|\mathbf{r}|\psi_{\mathbf{K}(t)}\rangle dt, \quad T=\frac{2\pi}{\omega},\end{aligned} \quad (5)$$

where in terms of the vector potential $\mathbf{A}(t)$ of $\mathbf{F}(t)$,

$$\mathbf{A}(t) = -\frac{c\mathcal{F}}{\omega}(\hat{\mathbf{x}}\sin\omega t - \hat{\mathbf{y}}\eta\cos\omega t), \quad (6)$$

we have

$$S(t,t_i) = \int_{t_i}^{t}\mathbf{K}^2(t';t,t_i)/(2m)dt', \quad (7)$$

$$\mathbf{K}(t';t,t_i) = \frac{|e|}{c}\left(\mathbf{A}(t') - \frac{\int_{t_i}^{t}\mathbf{A}(\tau)d\tau}{t-t_i}\right), \quad (8)$$

where $E = E_\Omega - |E_0|$, $a = \hbar^2/(me^2)$, $v_{\rm at} = e^2/\hbar$, $F_0 = \sqrt{8m|E_0|^3}/(|e|\hbar) = (\kappa a)^3F_{\rm at}$, $F_{\rm at} = |e|/a^2$, E_Ω is the harmonic energy, and $\mathbf{K}_i(t) \equiv \mathbf{K}(t_i;t,t_i)$, $\mathbf{K}(t) \equiv \mathbf{K}(t;t,t_i)$, where $\mathbf{K}(t';t,t_i)$ is the instantaneous (at time t') classical momentum of an electron that moves along a closed trajectory starting at time t_i and returning at time t. The wave function $\psi_{\mathbf{K}(t)}(\mathbf{r})$ is a field-free scattering state of an electron with "momentum" $\mathbf{K}(t)$ in TDER theory [35]. The integration in Eq. (5) extends over return times t of the electron over a half cycle $(T/2,T)$ of the field $\mathbf{F}(t)$. For a given t, the corresponding time $t_i = t_i(t)$ is determined as the root of the energy conservation equation applicable at the moment of ionization,

$$\mathbf{K}^2(t_i;t,t_i)/(2m) = -|E_0|, \quad (9)$$

that has a positive imaginary part and the smallest real part. Equation (9) is similar to that for the ionization time in the Keldysh theory of ionization [10]. It indicates that an adiabatic transition from a bound state to the continuum occurs at a complex moment of time, $t_i(t)$, when the energy of an electron in a laser field coincides with the energy E_0 [31]. Unlike in the Keldysh theory, in which the ionization time depends on the ionized electron's energy [10], in our case this time depends on the return time t (i.e., it is that time at which an electron begins its motion along a particular closed trajectory after tunneling such that it returns back to the tunnel exit point at the moment t [2]).

Note that the vector $\hat{\mathbf{K}}_i(t)$ lies in the polarization plane ($\theta = 90^\circ$), so that the kinematic factor $f_{1,0}[\hat{\mathbf{K}}(t)]$ in Eq. (5) is zero [cf. Eq. (4)] and HHG for the substate $\varphi_{\kappa 10}(\mathbf{r})$, which is oriented perpendicular to the polarization plane, is suppressed and vanishes in approximation (5). We emphasize also the significant difference between the dipole moment (5) and the SFA results [3,5]: the dipole moment $\mathbf{d}_{l,q}$ involves the exact photorecombination matrix element $\langle\varphi_{\kappa lq}|\mathbf{r}|\psi_{\mathbf{K}(t)}\rangle$ (within the TDER model [29]; see also Ref. [36]), while the SFA treats the corresponding matrix element in the plane wave (Born) approximation.

To present explicitly the dependence of the recombination matrix element in Eq. (5) on the vector $\mathbf{K}(t)$, we represent the wave function $\psi_{\mathbf{K}(t)}(\mathbf{r})$ by a partial wave expansion [31],

$$\psi_{\mathbf{K}(t)}(\mathbf{r}) = \sum_{l,m} \psi_{\epsilon(t),l}(r) Y^*_{l,m}[\hat{\mathbf{K}}(t)] Y_{l,m}(\hat{\mathbf{r}}), \tag{10}$$

$$\psi_{\epsilon(t),l}(r) = \frac{2\pi\hbar}{aK(t)} i^l e^{i\delta_l[\epsilon(t)]} R_{K(t),l}(r), \tag{11}$$

where $\epsilon(t) = K^2(t)/(2m)$, $R_{K(t),l}(r)$ is a continuum solution of the radial Schrödinger equation, and δ_l is its scattering phase. Carrying out the integration over the angular variables, we obtain

$$\langle\varphi_{\kappa,0,0}|\mathbf{r}|\psi_{\mathbf{K}(t)}\rangle = \frac{1}{\sqrt{4\pi}} \frac{\mathbf{K}(t)}{K(t)} D_{0,1}, \tag{12a}$$

$$\langle\varphi_{\kappa,1,+1}|x|\psi_{\mathbf{K}(t)}\rangle = i\sqrt{\frac{3}{4\pi}} \frac{K_x(t)K_y(t)}{K^2(t)} D_{1,2} \tag{12b}$$

$$\langle\varphi_{\kappa,1,+1}|y|\psi_{\mathbf{K}(t)}\rangle = i\sqrt{\frac{3}{4\pi}} \left[\frac{D_{1,0} - D_{1,2}}{3} + \frac{K_y^2(t)}{K^2(t)} D_{1,2}\right], \tag{12c}$$

$$\langle\varphi_{\kappa,1,-1}|x|\psi_{\mathbf{K}(t)}\rangle = -\sqrt{\frac{3}{4\pi}} \left[\frac{D_{1,0} - D_{1,2}}{3} + \frac{K_x^2(t)}{K^2(t)} D_{1,2}\right], \tag{12d}$$

$$\langle\varphi_{\kappa,1,-1}|y|\psi_{\mathbf{K}(t)}\rangle = -\sqrt{\frac{3}{4\pi}} \frac{K_x(t)K_y(t)}{K^2(t)} D_{1,2}, \tag{12e}$$

where $D_{l,l'} = \langle\varphi_{\kappa l}|r|\psi_{\epsilon(t),l'}\rangle$. In the TDER model, these radial matrix elements can be calculated explicitly using the field-free effective range wave functions,

$$D_{0,1} = 8\pi i C_{\kappa 0} \hbar^3 \sqrt{\kappa} \frac{K(t)}{[K^2(t) + (\hbar\kappa)^2]^2}, \tag{13a}$$

$$D_{1,0} = 4\pi C_{\kappa 1} \frac{\hbar^2}{\sqrt{\kappa}} \frac{K^2(t) + 3(\hbar\kappa)^2}{[K^2(t) + (\hbar\kappa)^2]^2}, \tag{13b}$$

$$D_{1,2} = -8\pi C_{\kappa 1} \frac{\hbar^2}{\sqrt{\kappa}} \frac{K^2(t)}{[K^2(t) + (\hbar\kappa)^2]^2}. \tag{13c}$$

The HHG amplitude (3) with $\mathbf{d}_{l,q}$ given by Eq. (5) generalizes the result for linear polarization [34] to the case of an elliptically polarized field. For $\eta \to 0$, only one dipole moment for each initial state becomes nonzero: $\mathbf{d}_{0,0}$ for an s state and $\mathbf{d}_{1,-1}$ for a p state, both of which are directed along the polarization vector of the field $\mathbf{F}(t)$. By using in Eq. (5) the explicit forms in Eq. (4) for $f_{l,q}[\hat{\mathbf{K}}(t)]$ as well as those in Eqs.(12) and (13) for the recombination matrix elements, it can be shown that the dipole moments $\mathbf{d}_{0,0}$ and $\mathbf{d}_{1,-1}$ given by Eq. (5) for $\eta = 0$ coincide with those given in Eq. (18) of Ref. [34]. Indeed, for $\eta = 0$ Eq. (9) can be written in the simple form,

$$K_{i,x}(t) = -i\hbar\kappa, \tag{14}$$

and the exact result for $K(t)$ [cf. Eq. (8) for $t' = t$] can then be approximated [using Eq. (14) and keeping only terms of order γ^{-1}] as follows:

$$K_x(t) = K_{i,x}(t) - \frac{\hbar\kappa}{\gamma}(\sin\omega t - \sin\omega t_i)$$
$$\approx -\frac{\hbar\kappa}{\gamma}(\sin\omega t - \sin\omega t_i), \quad K_y(t) = 0. \tag{15}$$

III. ANALYTIC EVALUATION OF THE DIPOLE MOMENT $\mathbf{d}_{l,q}$ IN THE PLATEAU CUTOFF REGION

A. General considerations for an arbitrary ellipticity η

To analyze the harmonic spectrum in the region near the plateau cutoff, we represent the dipole moment (5) in a more compact form,

$$\mathbf{d}_{l,q} = \int_{T/2}^{T} e^{-i\Phi(t)} \boldsymbol{g}(t) dt, \quad T = \frac{2\pi}{\omega}, \tag{16}$$

$$\boldsymbol{g}(t) = e \frac{2C_{\kappa,l}}{iT(\kappa a)^{3/2}} f_{l,q}[\hat{\mathbf{K}}_i(t)]$$
$$\times \left[\frac{\mathbf{F}(t_i)}{F_0} \cdot \frac{\mathbf{K}_i(t)}{\hbar\kappa}\right]^{-1/2} \frac{\langle\varphi_{\kappa lq}|\mathbf{r}|\psi_{\mathbf{K}(t)}\rangle}{[v_{\rm at}(t - t_i)]^{3/2}}, \tag{17}$$

$$\Phi(t) = [S(t,t_i) - Et + E_0 t_i]/\hbar. \tag{18}$$

In the quasiclassical limit ($\hbar\omega \ll |E_0|$), the phase factor $e^{-i\Phi(t)}$ in the integrand of Eq. (16) oscillates rapidly. Its main contributions come from the vicinity of each of the saddle points, $t = t_r$, satisfying the equation:

$$\left.\frac{d\Phi(t)}{dt}\right|_{t=t_r} = 0, \tag{19}$$

which gives explicitly [cf. Eqs. (7) and (18)],

$$\mathbf{K}^2(t_r)/(2m) = E. \tag{20}$$

The system of coupled equations (9) and (20) determines a set of quasiclassical closed electron trajectories ("electron orbits") in each of which the active electron is ionized at the moment t_i [cf. Eq. (9)] and returns at the moment t_r. The trajectories in this set have different travel times, but all of them correspond to the same energy E at the moment of

return. Moreover, the trajectories can be grouped in pairs ("short" and "long" orbits), with the trajectories of each pair merging into a single (extreme) one when the energy E approaches the value $E^s_{\max}$ corresponding to a local (sth) extremum of the function $\mathbf{K}^2(t)/(2m)$. Analysis shows that the largest of the local extrema, $E_{\max} = \max(E^s_{\max})$, is realized for the extreme trajectory with the smallest travel time, $\Delta t^{(0)} = t_r^{(0)} - t_i^{(0)}$. In what follows, we analyze only the region of the HHG spectrum near the plateau cutoff. Thus, we consider only those trajectories that are close to the extreme one described by the times $t_i^{(0)}$ and $t_r^{(0)}$ corresponding to $E_{\max}$. These times satisfy Eq. (9) and the following equation:

$$\left.\frac{d^2\Phi(t)}{d^2t}\right|_{t=t_r^{(0)}} = \left.\frac{\mathbf{K}(t)}{\hbar m}\frac{d}{dt}\mathbf{K}(t)\right|_{t=t_r^{(0)}} = 0. \tag{21}$$

To determine the times $t_r^{(0)}$ and $t_i^{(0)}$, we analyze first the extremum of the classical energy of an electron, $\mathcal{E}(t,t')$, moving along a closed trajectory (from time t' until the return time t) as a function of the two independent times, t' and t,

$$\mathcal{E}(t,t') = \frac{\mathbf{K}^2(t;t,t')}{2m} = \frac{K_x^2(t;t,t') + K_y^2(t;t,t')}{2m}. \tag{22}$$

Straightforward calculation of the partial derivatives of $\mathcal{E}(t,t')$ in t' and t respectively leads to the following system of equations for the classical times $t' = t_i^{\rm cl}$ and $t = t_r^{\rm cl}$:

$$k_x^r\left[\cos\tau_r + \frac{k_x^r}{\tau_r - \tau_i}\right] + k_y^r\left[\sin\tau_r + \frac{k_y^r}{\tau_r - \tau_i}\right] = 0, \tag{23a}$$

$$k_x^r k_x^i + k_y^r k_y^i = 0, \tag{23b}$$

where we have introduced the dimensionless times, $\tau_i = \omega t_i^{\rm cl}$ and $\tau_r = \omega t_r^{\rm cl}$, and the dimensionless momenta, $\mathbf{k}^r = \omega/(|e|\mathcal{F})\mathbf{K}(t_r^{\rm cl};t_r^{\rm cl},t_i^{\rm cl})$ and $\mathbf{k}^i = \omega/(|e|\mathcal{F})\mathbf{K}(t_i^{\rm cl};t_r^{\rm cl},t_i^{\rm cl})$,

$$k_x^r = -\left(\sin\tau_r + \frac{\cos\tau_r - \cos\tau_i}{\tau_r - \tau_i}\right), \tag{24}$$

$$k_y^r = \eta\left(\cos\tau_r - \frac{\sin\tau_r - \sin\tau_i}{\tau_r - \tau_i}\right), \tag{25}$$

$$k_x^i = -\left(\sin\tau_i + \frac{\cos\tau_r - \cos\tau_i}{\tau_r - \tau_i}\right), \tag{26}$$

$$k_y^i = \eta\left(\cos\tau_i - \frac{\sin\tau_r - \sin\tau_i}{\tau_r - \tau_i}\right). \tag{27}$$

The system of equations (23) is equivalent to each of the following two sets of equations:

$$k_x^i = 0, \quad k_y^r = 0, \tag{28a}$$

$$k_y^i = 0, \quad k_x^r = 0. \tag{28b}$$

The set of equations (28a) has a transparent physical meaning: $k_x^i = 0$ means that the electron starts to move along a closed trajectory with zero velocity along the x axis (while the y component is not zero in general); the second equation implies that the electron returns to the starting point with zero momentum along the y axis (while its x component is not zero at the return time). The electron thus moves along an extreme trajectory, making a petal-like loop. Note that Eqs. (28a) coincide with similar ones for linear polarization [34] and have the same solutions: $\tau_i = 0.313$, $\tau_r = 4.399$. The corresponding maximum energy is

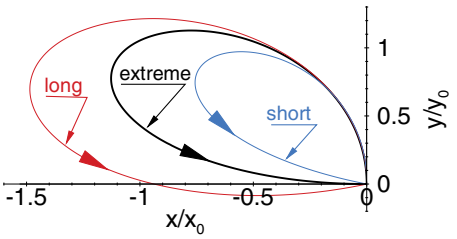

FIG. 1. (Color online) Schematic sketch of short, long, and extreme trajectories, with the arrows indicating the direction of propagation. The coordinates are scaled in units of $x_0 = |e|\mathcal{F}/(m\omega^2)$ and $y_0 = \eta x_0$.

$$\mathcal{E}_{\max} = \mathcal{E}_0/(1+\eta^2), \quad \mathcal{E}_0 = 2(\sin\tau_r - \sin\tau_i)^2 u_p \approx 3.17u_p, \tag{29}$$

where $u_p = e^2F^2/(4m\omega^2)$. The extreme trajectory, as well as the corresponding short and long trajectories, are shown in Fig. 1. The set of equations (28b) also describes a petal-like loop trajectory; however, this trajectory contributes to the low-energy part of the HHG spectrum (since the energy at the moment of return is proportional to the parameter η^2, which we will consider later as a small parameter). Thus we do not consider the solutions of this system in detail.

B. Approximate analysis for small η

The solutions of the classical Eqs. (28a) can be used as zero-order approximations to the ionization and recombination times $t_i^{(0)}$ and $t_r^{(0)}$ corresponding to the coalescence points of short and long trajectories: $\omega t_i^{(0)} \approx \tau_i$ and $\omega t_r^{(0)} \approx \tau_r$. To find the quantum corrections to τ_i and τ_r, we rewrite Eq. (9) explicitly for $t = t_r^{(0)}$ and $t_i = t_i^{(0)}$,

$$\left[\sin\omega t_i^{(0)} + \frac{\cos\omega t_r^{(0)} - \cos\omega t_i^{(0)}}{\omega\left(t_r^{(0)} - t_i^{(0)}\right)}\right]^2 = -\gamma^2(1+\eta^2) - \eta^2\left[\cos\omega t_i^{(0)} - \frac{\sin\omega t_r^{(0)} - \sin\omega t_i^{(0)}}{\omega\left(t_r^{(0)} - t_i^{(0)}\right)}\right]^2, \tag{30}$$

where $\gamma \ll 1$. Assuming also $\eta^2 \ll 1$ and neglecting the term $\sim\eta^2\gamma^2$, we consider the right-hand side of Eq. (30) as a perturbation. Thus Eq. (30) can be solved iteratively, in a way similar to that employed in Ref. [34],

$$\omega t_i^{(0)} \approx \tau_i + i\Delta_i, \quad \Delta_i = \tilde{\eta}\frac{\cos\tau_i - \cos\tau_r}{\cos\tau_i}, \tag{31}$$

$$\tilde{\eta} = \sqrt{\eta^2 + |E_0|/\mathcal{E}_0}. \tag{32}$$

The lowest-order corrections to the recombination time $t_r^{(0)} = \tau_r/\omega$ (not shown) are of the order of η^2 and γ^2; we thus omit these corrections in our calculations since we find numerically that their contributions to the final results are negligible. Taking into account the quantum correction Δ_i to the ionization time and approximating the classical energy $\mathcal{E}_{\max}$ by $\mathcal{E}_{\max} \approx \mathcal{E}_0(1-\eta^2)$, the maximum energy, $E_{\max}$, can be found as

in Ref. [34],

$$E_{\max} = \max\left[\mathcal{E}\left(t_i^{(0)},t_r^{(0)}\right)\right] \approx \mathcal{E}_0(1-\eta^2) + 0.324|E_0|\alpha_0^2, \tag{33}$$

$$\alpha_0 = \tilde{\eta}\sqrt{\mathcal{E}_0/|E_0|} = \sqrt{1+\eta^2\mathcal{E}_0/|E_0|}. \tag{34}$$

Returning to the evaluation of the integral in Eq. (16), taking into account Eq. (21), we approximate the phase $\Phi(t)$ in the vicinity of the point $t = t_r^{(0)} \approx \tau_r/\omega$ by a cubic polynomial,

$$\Phi(t) \approx \Phi\left(t_r^{(0)}\right) + \frac{(E_{\max}-E)}{\hbar}\left(t-t_r^{(0)}\right) - \frac{\tilde{\delta}}{3}\left(t-t_r^{(0)}\right)^3, \qquad \tilde{\delta} = -\frac{1}{2}\frac{d^3\Phi(t)}{dt^3}\bigg|_{t=t_r^{(0)}}, \tag{35}$$

where it can be shown that $\tilde{\delta} > 0$. For a small ellipticity, $\tilde{\delta}$ can be calculated as was done for the case of linear polarization in Ref. [34],

$$\tilde{\delta} = \omega_{\rm at}^3\left(\frac{I\delta}{2I_{\rm at}}\right), \qquad \delta = \cos^2\tau_r\left[\frac{\sin\tau_r}{\cos\tau_r}(\tau_r-\tau_i) + \frac{\cos\tau_r}{\cos\tau_i} - 1\right] \approx 1.072, \tag{36}$$

where $I = cF^2/(8\pi)$, $I_{\rm at} = cF_{\rm at}^2/(8\pi)$, $\omega_{\rm at} = E_{\rm at}/\hbar$, and $E_{\rm at} = e^2/a$.

In the cubic approximation for $\Phi(t)$, Eq. (20) reduces to a quadratic equation for the recombination times, whose roots are given by

$$t_r^{\pm} = t_r^{(0)} \pm \beta, \quad \beta = \sqrt{\frac{E_{\max}-E}{\hbar\tilde{\delta}}}, \tag{37}$$

where β is a small parameter. The complex ionization times, $t_i^{\pm}$, corresponding to the recombination times $t_r^{\pm}$, can be found as

$$t_i^{\pm} = t_i^{(0)} + \frac{\partial t_i}{\partial t}\bigg|_{t=t_r^{(0)}}\frac{\partial t_r^{\pm}}{\partial\beta}\beta. \tag{38}$$

By taking into account the derivative $\partial t_i/\partial t$ for $t = t_r^{(0)}$, which can be found by differentiating Eq. (9) in t, we obtain that

$$\frac{\partial t_i}{\partial t}\bigg|_{t=t_r^{(0)}} \approx \frac{\cos\tau_r}{\cos\tau_i}\left(1 + i\,\Delta_i\tan\tau_i\right), \tag{39}$$

$$\tan\tau_i = -\frac{\cos\tau_r}{\cos\tau_i} \approx 0.324, \tag{40}$$

$$\omega t_i^{\pm} = \tau_i + i\,\Delta_i \pm \frac{\cos\tau_r}{\cos\tau_i}\omega\beta\left(1 + i\,\Delta_i\tan\tau_i\right). \tag{41}$$

Finally, the evaluation of the integral in Eq. (16) can be carried out using the saddle-point method for two coalescing saddle points (which are t_r^+ and t_r^- in our case) [37]

$$\int_{T/2}^{T} e^{-i\Phi(t)}\boldsymbol{g}(t)dt \approx 2\pi\tilde{\delta}^{-1/3}e^{-i\Phi(t_r^{(0)})}\left[\frac{\boldsymbol{g}(t_r^+)+\boldsymbol{g}(t_r^-)}{2}\mathrm{Ai}\,(\zeta) - i\,\frac{\boldsymbol{g}(t_r^+)-\boldsymbol{g}(t_r^-)}{2\beta\tilde{\delta}^{1/3}}\mathrm{Ai}'(\zeta)\right], \tag{42}$$

where $\mathrm{Ai}(\zeta)$ and $\mathrm{Ai}'(\zeta)$ are an Airy function and its derivative,

$$\zeta = -\left\{\frac{3}{4}[\Phi(t_r^+) - \Phi(t_r^-)]\right\}^{2/3} = \frac{E-E_{\max}}{\varrho E_{\rm at}}, \tag{43}$$

$$\varrho = \left(\frac{\delta I}{2I_{\rm at}}\right)^{1/3} \approx \left(0.536\frac{I}{I_{\rm at}}\right)^{1/3}, \tag{44}$$

$$\Phi\left(t_r^{(0)}\right) = \frac{1}{\hbar}\left[\int_{t_i^{(0)}}^{t_r^{(0)}}\frac{\mathbf{K}^2\left(t';t_r^{(0)},t_i^{(0)}\right)}{2m}dt' - Et_r^{(0)} + E_0t_i^{(0)}\right] \approx \mathrm{Re}\,\Phi\left(t_r^{(0)}\right) - i\frac{F_0\alpha_0^3}{3F\cos\tau_i}, \tag{45}$$

where $t_i^{(0)}$ is given by Eq. (31) and $t_r^{(0)} = \tau_r/\omega$. To evaluate accurately the vector function $\boldsymbol{g}(t_r^{\pm})$, we calculate the vectors $\mathbf{K}_i(t_r^{\pm}) \equiv (K_{ix},K_{iy})$ and $\mathbf{K}(t_r^{\pm}) \equiv (K_x,K_y)$ including corrections up to the order of η, $\tilde{\eta}$, β, and $\beta\tilde{\eta}$,

$$\mathbf{K}_i(t_r^{\pm}) \approx (-i\hbar\kappa\alpha_0, \eta\sqrt{2m\mathcal{E}_0}), \qquad \mathbf{K}(t_r^{\pm}) \approx \sqrt{2mE}\left(1, \eta\sqrt{\frac{2u_p}{E}}[i\varkappa_0 \pm \varkappa_1\delta^{1/2}\omega\beta]\right), \tag{46}$$

where

$$\varkappa_0 = \Delta_i\sin\tau_i \approx 0.408\tilde{\eta},$$
$$\varkappa_1 = \delta^{-1/2}\left\{-\frac{\sin(\tau_r-\tau_i)}{\cos\tau_i} + i\,\Delta_i\sin\tau_i \times\left[\tan\tau_i\frac{\cos\tau_r}{\cos\tau_i} + \frac{1}{\tau_r-\tau_i}\left(\frac{\cos\tau_r}{\cos\tau_i}-1\right)\right]\right\} \approx 0.822 - i0.169\tilde{\eta}. \tag{47}$$

We also approximate $t_r^{\pm} - t_i^{\pm} \approx (\tau_r-\tau_i)/\omega \equiv \Delta t$, $[\mathbf{F}(t_i^{\pm})\cdot\mathbf{K}_i(t_r^{\pm})] \approx -iF\hbar\kappa\alpha_0\cos\tau_i$. With these approximations, we obtain

$$\frac{\boldsymbol{g}(t_r^+)+\boldsymbol{g}(t_r^-)}{2} \approx \mathcal{C}_{l,q}\left(1, i\eta\varkappa_0\sqrt{\frac{2u_p}{E}}\right)\hat{\mathcal{S}}_{l,q}, \tag{48}$$

$$\frac{\boldsymbol{g}(t_r^+)-\boldsymbol{g}(t_r^-)}{2\omega\beta} \approx \mathcal{C}_{l,q}\left(0, \eta\varkappa_1\sqrt{\frac{2\delta u_p}{E}}\right)\hat{\mathcal{S}}_{l,q}, \tag{49}$$

where

$$\mathcal{C}_{l,q} = \frac{C_{\kappa l}\omega_{\rm at}}{4\pi^2}\sqrt{\frac{\kappa a}{\alpha_0\cos\tau_i}}\gamma\sqrt{\frac{F}{F_0}}\frac{\tilde{f}_{l,q}}{(v_{\rm at}\Delta t)^{3/2}}, \tag{50}$$

$\tilde{f}_{0,0} = 1$, $\tilde{f}_{1,-1} = \alpha_0$, $\tilde{f}_{1,1} = i\eta\sqrt{\mathcal{E}_0/|E_0|} = i\sqrt{\alpha_0^2-1}$, and $\hat{\mathcal{S}}_{l,q}$ is a 2×2 matrix,

$$\hat{\mathcal{S}}_{0,0} = D_{0,1}\begin{pmatrix}1&0\\0&1\end{pmatrix}, \quad \hat{\mathcal{S}}_{1,+1} = \begin{pmatrix}0 & D_{1,0}-D_{1,2}\\ 3D_{1,2} & 0\end{pmatrix}, \qquad \hat{\mathcal{S}}_{1,-1} = \begin{pmatrix}D_{1,0}+2D_{1,2} & 0\\ 0 & 3D_{1,2}\end{pmatrix}. \tag{51}$$

In Eqs. (48) and (49) we have neglected terms of order $\sim\eta^2$.

C. Analytic small-η result for $\mathbf{d}_{l,q}$

Taking into account Eqs. (42)–(51), we obtain analytic results for both components of the dipole moment $\mathbf{d}_{l,q}$ (i.e.,

$d_x^{(l,q)}$ and $d_y^{(l,q)}$) that are valid for small ellipticity η, i.e., approximating $\mathcal{E}_{\max} \approx \mathcal{E}_0(1-\eta^2)$ and assuming a characteristic parameter of the problem, given by Eq. (32), is small,

$$\tilde{\eta} \equiv \sqrt{\eta^2 + |E_0|/\mathcal{E}_0} \ll 1. \tag{52}$$

The result for the (two-dimensional) vector $\mathbf{d}_{l,q} = (d_x^{(l,q)}, d_y^{(l,q)})$ has scalar, vector, and matrix factors,

$$\mathbf{d}_{l,q} = e\mathcal{T}_{l,q}\boldsymbol{\chi}\hat{\mathcal{S}}_{l,q}. \tag{53}$$

The factor $\mathcal{T}_{l,q}$ is a scalar describing the tunneling of the electron from the state $\varphi_{\kappa lq}(\mathbf{r})$ at the time $t = t_i^{\rm cl} \equiv \tau_i/\omega \approx 0.05T$ with "transverse" momentum $\mathbf{p}_i = \eta\sqrt{2m\mathcal{E}_0}\,\hat{\mathbf{y}}$,

$$\mathcal{T}_{l,q} = \frac{\tilde{f}_{l,q}}{\pi\alpha_0^2}\tilde{\gamma}\sqrt{\frac{\Gamma_{\rm st}(\tilde{F})}{(2l+1)\kappa v_{\rm at}}}, \tag{54}$$

$$\Gamma_{\rm st}(\tilde{F}) = \frac{|E_0|}{\hbar}(2l+1)C_{\kappa l}^2\frac{\tilde{F}}{2F_0}e^{-2F_0/(3\tilde{F})},$$

$$\alpha_0 = \sqrt{1+\eta^2\mathcal{E}_0/|E_0|} = \tilde{\eta}\sqrt{\mathcal{E}_0/|E_0|}, \tag{55}$$

$$\tilde{F} \equiv F\cos\left(\omega t_i^{\rm cl}\right)\big/\alpha_0^3 \approx 0.95F/\alpha_0^3, \quad \tilde{\gamma} = \hbar\omega\kappa/(|e|\tilde{F}),$$

where $\tilde{f}_{0,0} = 1$, $\tilde{f}_{1,-1} = \alpha_0$, $\tilde{f}_{1,1} = i\eta\sqrt{\mathcal{E}_0/|E_0|} = i\sqrt{\alpha_0^2-1}$, and $\Gamma_{st}(\tilde{F})$ is the detachment rate for a state $\varphi_{\kappa lm=0}(\mathbf{r})$ in a static electric field of strength $\tilde{F}\hat{\mathbf{z}}$ [38].

The factor $\boldsymbol{\chi}$ in Eq. (53) is a vector, $\boldsymbol{\chi} = (\chi_x, \chi_y)$, *independent* of the symmetry of the state $\varphi_{klq}(\mathbf{r})$,

$$\chi_x = \mathcal{D}\mathrm{Ai}(\zeta), \quad \zeta = \frac{E - E_{\max}}{\varrho E_{\rm at}}, \tag{56}$$

$$\chi_y = i\eta\mathcal{D}\left[\varkappa_0\sqrt{\frac{2u_p}{E}}\mathrm{Ai}(\zeta) - \varkappa_1\sqrt{\frac{\varrho E_{\rm at}}{E}}\mathrm{Ai}'(\zeta)\right], \tag{57}$$

$$E_{\max} = \mathcal{E}_0(1-\eta^2) + \Delta, \quad \Delta \approx 0.324|E_0|\alpha_0^2,$$

$$\varkappa_0 \approx 0.408\tilde{\eta}, \quad \varkappa_1 \approx 0.822 - i0.169\tilde{\eta},$$

$$\mathcal{D} = \frac{1}{\varrho(v_{\rm at}\Delta t)^{3/2}}e^{-i\Phi_0}, \quad \varrho = \left(0.536\frac{I}{I_{\rm at}}\right)^{1/3}, \tag{58}$$

$$\Delta t = t_r^{\rm cl} - t_i^{\rm cl} \approx 0.65T, \quad I = cF^2/(8\pi),$$

$$\Phi_0 = \left[S\left(t_r^{\rm cl}, t_i^{\rm cl}\right) + E_0 t_i^{\rm cl} - Et_r^{\rm cl}\right]\big/\hbar + 3\pi/4,$$

where $E_{\rm at} = 27.21$ eV and $I_{\rm at} = 3.51\times10^{16}$ W/cm^2. The term Δ in Eq. (58) generalizes the quantum correction to the classical cutoff law for a linearly polarized field [39] to the case of a small ellipticity η. The components χ_x and χ_y are insensitive to the atomic dynamics and describe propagation of an electron in the laser field over the time interval Δt from ionization to recombination. For $\eta = 0$, we have $\chi_y = 0$, and χ_x coincides with the propagation amplitude for a linearly polarized field [34]. As for the case $\eta = 0$, the Airy functions in Eqs. (56), (57) describe the interference of short and long trajectories in the region below the plateau cutoff, $E < E_{\max}$ (i.e., $\zeta < 0$), from which originate the typical oscillation patterns in the HHG yield.

The last factor in the parametrization (53), $\hat{\mathcal{S}}_{l,q}$, is a 2×2 matrix (51) that describes the recombination step of an HHG process. Its matrix elements do not depend on laser parameters and involve only radial matrix elements $D_{l,l'} = \langle\varphi_{\kappa l}|r|\psi_{E,l'}\rangle$, where $\psi_{E,l'}(r)$ is the radial part of the l'-wave component (including the phase factor $\exp[i\delta_{l'}(E)]$) of the scattering state $\psi_{\mathbf{p}}(\mathbf{r})$ [cf. Eq. (11)]. (Note that the matrix elements $D_{l,l'}$ become real in the plane-wave approximation.) For an initial s state, the matrix $\hat{\mathcal{S}}_{l,q}$ is diagonal, while for a p state this matrix has different forms for $q = \pm1$ [cf. Eq. (51)]. Matrix elements of $\hat{\mathcal{S}}_{l,q}$ are related to the PRCS, $\sigma(E,\alpha)$, for emission of a photon with its linear polarization vector oriented at an angle α to the momentum of the recombining electron. For recombination to an s state,

$$\sigma_s(E,\alpha) = \frac{\hbar\Omega^3}{8\pi^2apc^3}|D_{0,1}|^2\cos^2\alpha, \quad p = \sqrt{2mE}, \tag{59}$$

while for recombination to a p state we have

$$\sigma_p(E,0^\circ) = \frac{\hbar\Omega^3}{24\pi^2apc^3}|D_{1,0} + 2D_{1,2}|^2, \tag{60}$$

$$\sigma_p(E,90^\circ) = \frac{\hbar\Omega^3}{24\pi^2apc^3}|D_{1,0} - D_{1,2}|^2. \tag{61}$$

IV. APPLICATION TO HHG RATES FOR NEUTRAL ATOMS

Since each of the three factors in (53) has a clear physical meaning in terms of the three-step HHG scenario [40,41] and since $\boldsymbol{\chi}$ is insensitive to atomic dynamics, we extend the parametrization (53) to the case of a neutral atom by replacing the tunneling rate $\Gamma_{\rm st}(\tilde{F})$ and matrix elements $D_{l,l'}$ [or $\sigma(E,\alpha)$] by their counterparts for a given atom (cf. Ref. [26]). In what follows, we discuss HHG from bound s and p states separately.

A. HHG rates for initial s states

For an initial s state ($l = 0$), the harmonic rate, $\mathcal{R}_s(E_\Omega)$, can be presented in a factorized form similar to that in Ref. [26] for the case of linear polarization,

$$\mathcal{R}_s(E_\Omega) = \mathcal{I}(\tilde{F},\omega)\mathcal{W}(E)\sigma_s(E,0^\circ), \tag{62}$$

where $\mathcal{I}(\tilde{F},\omega) = 4\pi|\mathcal{T}_{0,0}|^2$ is the ionization factor and $\mathcal{W}(E) = p(|\chi_x|^2 + |\chi_y|^2)/m$ is the propagation factor. The factorization (62) provides a quantum-mechanical justification for the Gaussian dependence of the HHG yield on the ellipticity obtained semiclassically [13]. Indeed, for small η, the factor $\mathcal{W}(E)$ in Eq. (62) is well approximated by its value for $\eta = 0$, while the exponent of $\Gamma_{\rm st}$ in Eq. (55) can be expanded in a series in the parameter η^2. Taking into account the term $\sim\eta^2$ in this expansion, we recover Eq. (6) of Ref. [13]. (Note that the η^2 expansion converges only for $\eta^2\mathcal{E}_0/|E_0| < 1$.)

For small η, the contribution of the component $d_y^{(0,0)}$ to the HHG yield is small. However, this component governs the polarization of the harmonics. In particular, the degree of circular polarization, ξ_s [which is related to the ellipticity η_s according to $\xi_s = 2\eta_s/(1+\eta_s^2)$], equals

$$\xi_s = 2\mathrm{Im}\left(d_x^{(0,0)*}d_y^{(0,0)}\right)\big/|\mathbf{d}_{0,0}|^2. \tag{63}$$

The general result (63) for an s state simplifies in the plateau cutoff region, where both $d_x^{(0,0)}$ and $d_y^{(0,0)}$ involve the same factors $\mathcal{T}_{0,0}$ and $\hat{\mathcal{S}}_{0,0}$, which cancel in the ratio (63) [i.e., ξ_s may be obtained from Eq. (63) by substituting $d_x^{(0,0)} \to \chi_x$ and $d_y^{(0,0)} \to \chi_y$]. Thus, ξ_s is proportional to η and does not

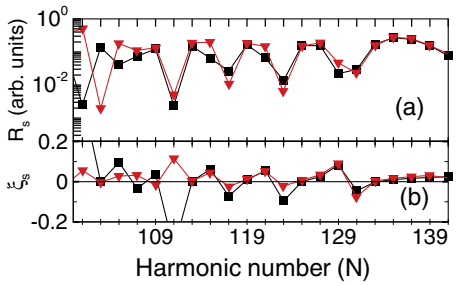

FIG. 2. (Color online) (a) The rate, $\mathcal{R}_s(E_\Omega)$, and (b) the degree of circular polarization, ξ_s, of harmonics for an s state with energy $E_0 = -15.76$ eV in a laser field with intensity $I = 2.2 \times 10^{14}$ W/cm^2, wavelength $\lambda = 1.3\,\mu$m, and ellipticity $\eta = 0.1$. Squares: TDSE results [19]; triangles: Eqs. (62) and (63).

depend on the atomic dynamics, in agreement with numerical results for an s state [19].

In Fig. 2 we compare numerical results of TDSE calculations [19] with the analytic results (62) and (63). The agreement is excellent in the plateau-cutoff region, where the factorization (62) is valid. The oscillation pattern in the dependence of ξ_s on N [cf. Fig. 2(b)] originates from interference of short and long trajectories and reflects the interference oscillations of the rates that one observes in Fig. 2(a).

B. HHG rates for initial p states

For an initial p state, two substates (with $q = \pm 1$) contribute to the HHG rate and polarization parameters,

$$\mathcal{R}_p = \mathcal{R}_+ + \mathcal{R}_-, \quad \xi_p = (\xi_+\mathcal{R}_+ + \xi_-\mathcal{R}_-)/\mathcal{R}_p, \tag{64}$$

where $\mathcal{R}_\pm \propto |\mathbf{d}_{1,\pm1}|^2$ are partial HHG rates for substates $\varphi_{\kappa lq}(\mathbf{r})$ with $q = \pm 1$, and $\xi_\pm$ are given by Eq. (63) with the replacements $\mathbf{d}_{0,0} \to \mathbf{d}_{1,\pm1}$. In Fig. 3 we show the excellent agreement between exact TDER results for $\mathcal{R}_p$ and ξ_p and those calculated using Eq. (53). We emphasize a number of major differences between HHG from s and p states: (i) the rate $\mathcal{R}_p$ cannot be factorized as a product of laser and atomic parameters since the matrix $\hat{\mathcal{S}}_{1,q}$ in Eq. (51) has different components for $q = \pm 1$, which cannot be combined into a single atomic factor in the rate $\mathcal{R}_p$; (ii) for a p state, the emitted harmonics are only partially polarized due to an incoherent

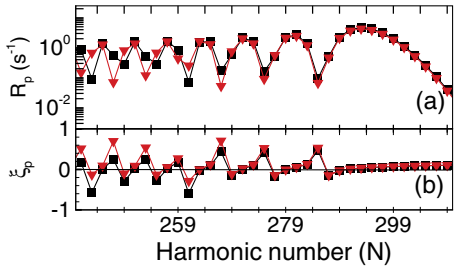

FIG. 3. (Color online) (a) The rate, $\mathcal{R}_p$, and (b) the circular polarization degree, ξ_p, of harmonics produced by a p state with energy $E_0 = -12.13$ eV for a laser intensity $I = 2 \times 10^{14}$ W/cm^2, wavelength $\lambda = 1.8\mu$m, and ellipticity $\eta = 0.1$. Squares: exact TDER results; triangles: results obtained using the parametrization (53) and Eq. (64).

contribution of two degenerate substates with $q = \pm 1$ [cf. Eq. (64)] [42]; and (iii) the circular polarization degree ξ_p becomes dependent on the atomic structure even for a small ellipticity.

The results in Eq. (53) are valid for small η and γ, while the ratio $r = (\eta/\gamma)^2$ may be arbitrary. This ratio governs the relative contributions of the ionization factors $\mathcal{T}_{1,\pm1}$ to the dipole moments $\mathbf{d}_{1,\pm1}$,

$$|\mathcal{T}_{1,+1}|/\mathcal{T}_{1,-1} = \sqrt{\alpha_0^2 - 1}/\alpha_0 \approx \sqrt{1.6r/(1+1.6r)}. \tag{65}$$

Note that χ_y contributes negligibly to the partial rates $\mathcal{R}_\pm$ owing to the smallness of the ratio $|\chi_y/\chi_x| \propto \eta$. Thus, after neglecting the component χ_y of the vector $\boldsymbol{\chi}$, the rate (2) summed over polarizations of the harmonic photon can be expressed as a sum of two terms,

$$\mathcal{R}_p \approx \mathcal{R}_x + \mathcal{R}_y = W^{(-1)}\sigma(E,0^\circ) + W^{(+1)}\sigma(E,90^\circ), \tag{66}$$

where the EWPs $W^{(\pm1)}$ are defined by

$$W^{(\pm1)} = 4\pi p|\mathcal{T}_{1,\pm1}\chi_x|^2/m. \tag{67}$$

For the case $\eta \ll \gamma$, $W^{(+1)} \ll W^{(-1)}$ [cf. Eq. (65)], so that only a single state, $\varphi_{\kappa lq=-1}(\mathbf{r})$ (i.e., the component $d_x^{(1,-1)}$ of $\mathbf{d}_{1,-1}$), contributes to the rate (66),

$$\mathcal{R}_p \approx \mathcal{R}_x = W^{(-1)}\sigma(E,0^\circ). \tag{68}$$

Thus, the rate $\mathcal{R}_p$ has a factorized form with EWP $W^{(-1)}$, while the parameter $\xi_p \approx \xi_-$, so that the harmonics are completely polarized.

For the case $\eta \lesssim \gamma$, which can be realized for intense midinfrared lasers [43,44], both dipoles, $\mathbf{d}_{1,-1}$ and $\mathbf{d}_{1,+1}$(i.e., $d_x^{(1,-1)}$ and $d_y^{(1,+1)}$), contribute to the rate (66). Moreover, the components $d_x^{(1,-1)}$ and $d_y^{(1,+1)}$ determine the yield of harmonics linearly polarized in orthogonal directions: $\hat{\mathbf{x}}$ (with rate $\mathcal{R}_x$) and $\hat{\mathbf{y}}$ (with rate $\mathcal{R}_y$). This selectivity allows one to obtain from HHG spectra complete information on the PRCS, i.e., the angle-integrated PRCS σ_0 and the asymmetry parameter β [28],

$$\sigma(E,\alpha) = \frac{\sigma_0}{4\pi}\left(1 + \beta\frac{3\cos^2\alpha - 1}{2}\right). \tag{69}$$

Indeed, measuring the ratio of intensities for harmonics linearly polarized in $\hat{\mathbf{y}}$ and $\hat{\mathbf{x}}$ directions (i.e., $\mathcal{R}_y/\mathcal{R}_x$) we calculate the ratio, $\wp \equiv \sigma(E,90^\circ)/\sigma(E,0^\circ)$ as [cf. Eqs. (65), (67)]

$$\wp = \frac{W^{(-1)}}{W^{(+1)}}\frac{\mathcal{R}_y}{\mathcal{R}_x} = \frac{\alpha_0^2}{\alpha_0^2 - 1}\frac{\mathcal{R}_y}{\mathcal{R}_x}. \tag{70}$$

From Eq. (69), β can be determined from $\wp$,

$$\beta = (1 - \wp)/(\wp + 1/2), \tag{71}$$

and σ_0 [$= 4\pi\sigma(E,0^\circ)/(1+\beta)$] can then be obtained using the measured value of $\mathcal{R}_x$:

$$\sigma_0 = 4\pi\mathcal{R}_x/[(1+\beta)W^{(-1)}]. \tag{72}$$

To illustrate the above algorithm, we consider HHG for Xe in a midinfrared ($\lambda = 1.8\mu$m) laser field with ellipticity $\eta = 0.1$. To obtain the photorecombination data for Xe, we use theoretical photoionization data [45] and the principle of detailed balance. In Figs. 4(a) and 4(b), we present theoretical

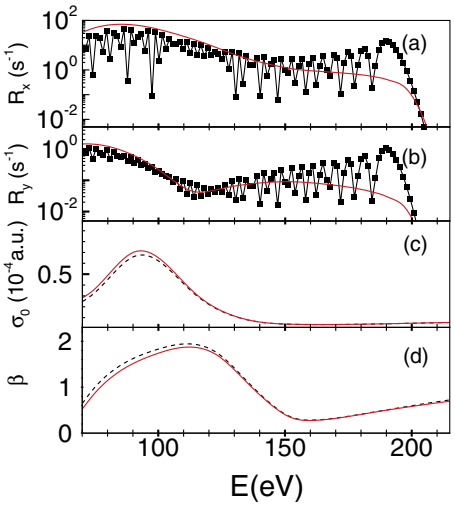

FIG. 4. (Color online) (a) The rates $\mathcal{R}_x$ and (b) $\mathcal{R}_y$ vs the recombining electron energy E ($= E_\Omega - |E_0|$) for HHG of Xe in a laser field with $\lambda = 1.8\mu$m and $\eta = 0.1$. Black squares: results for a laser intensity $I = 2 \times 10^{14}$ W/cm^2 obtained using Eq. (64); solid (red) lines: focal-averaged results (see text) for a peak intensity $I_0 = 2.1 \times 10^{14}$ W/cm^2. (c) The total PRCS $\sigma_0(E)$ and (d) the asymmetry parameter $\beta(E)$ for Xe. Dashed lines: theoretical results extracted from Ref. [45]; solid lines: results extracted from the focal-averaged HHG spectra in (a) and (b) using Eqs. (70), (71), and (72).

results for $\mathcal{R}_x$ and $\mathcal{R}_y$ obtained using Eq. (64) for a laser intensity $I = 2 \times 10^{14}$ W/cm^2. In order to smooth the oscillatory pattern of the rates $\mathcal{R}_{x,y}$, we also present in Figs. 4(a) and 4(b) focal averaged rates, obtained similarly to the procedure used in Ref. [48], assuming a Gaussian distribution of laser intensity with a peak value $I_0 = 2.1 \times 10^{14}$ W/cm^2. After focal averaging, we used the algorithm described above to retrieve β and σ_0 [cf. Eqs. (71) and (72)]. As shown in Figs. 4(c) and 4(d), the retrieved values of β and σ_0 agree very well with those extracted from Ref. [45]. This thus indicates that focal averaging does not prevent the retrieval of PRCS data from HHG spectra produced in a focused laser beam.

V. DISCUSSION AND CONCLUSION

Besides providing a means to retrieve field-free dynamical information on target atoms or molecules, such as the PRCS (which, of course, can also be obtained using more traditional techniques), HHG spectroscopy has a fundamental interest since it provides important information for a better understanding of the physics of strong field processes. In particular, HHG-spectroscopy experiments have shown that HHG spectra are clearly sensitive to details of field-free atomic dynamics, such as the Cooper minimum in the photoionization cross section [46,47]. Moreover, based on the theoretical factorization of the HHG yield in the high-energy region of the HHG spectrum, the importance of essentially multielectron atomic dynamics in strong field processes (such as the giant dipole resonance in the photoionization cross section of Xe) was predicted [26] and measured [24]. As we have shown in this paper, the capability of existing methods of linear HHG spectroscopy (i.e., using linearly polarized fields) can be significantly extended by elliptic HHG spectroscopy (i.e., using a laser field with nonzero ellipticity). Our results show that the principal feature of HHG in a laser field with nonzero ellipticity is its sensitive dependence on the spatial symmetry of the bound electron wave function: the electron density in s states is spherically symmetric, while that for states with $l > 0$ breaks the spherical symmetry. Consequently, we have shown theoretically that the HHG yield for s states can be factorized in terms of an EWP and the PRCS $\sigma_s(E,0^\circ)$, from which one can obtain $\sigma_s(E,\alpha)$ using Eq. (59). For p states factorization is generally impossible since both $\sigma_p(E,0^\circ)$ and $\sigma_p(E,90^\circ)$ contribute to the HHG yield. Nevertheless, polarization measurements within elliptic HHG spectroscopy permit one to retrieve both the energy and angular dependence of the PRCS $\sigma_p(E,\alpha)$.

Finally, we note that the analysis of HHG presented in this paper for a nonzero driving laser ellipticity is valid for atomic systems. Owing to the spherical symmetry of the atom, the polarization of harmonics generated by atoms remains linear for a linearly polarized laser field. For molecules, which in general do not have spherical symmetry, harmonics can be elliptically polarized even for a linearly polarized pump field. It is thus an interesting question what additional information on field-free molecular dynamics can be obtained by using an elliptically polarized driving laser field. However, the answer to this question requires a separate analysis.

ACKNOWLEDGMENTS

We thank M.Yu. Ivanov for helpful discussions and M.Yu. Ryabikin for providing the TDSE results in Fig. 2. This work was supported in part by RFBR Grants No. 12-02-12101-ofi_m and No. 13-02-00420-a, by NSF Grant No. PHY-1208059, by the Russian Federation Ministry of Education and Science, and by a grant from the Strategic Development Program of Voronezh State University (T.S.S.).

[1] N. L. Manakov and V. D. Ovsiannikov, Zh. Eksp. Teor. Fiz. **79**, 1769 (1980) [Sov. Phys. JETP **52**, 895 (1980)].
[2] P. Antoine, A. L'Huillier, M. Lewenstein, P. Salières, and B. Carré, Phys. Rev. A **53**, 1725 (1996).
[3] M. Y. Ivanov, T. Brabec, and N. Burnett, Phys. Rev. A **54**, 742 (1996).
[4] N. L. Manakov, Zh. Eksp. Teor. Fiz. **110**, 1244 (1996) [Sov. Phys. JETP **83**, 685 (1996)].
[5] P. Antoine, B. Carré, A. L'Huillier, and M. Lewenstein, Phys. Rev. A **55**, 1314 (1997).
[6] W. Becker, A. Lohr, M. Kleber, and M. Lewenstein, Phys. Rev. A **56**, 645 (1997).

[7] F. A. Weihe, S. K. Dutta, G. Korn, D. Du, P. H. Bucksbaum, and P. L. Shkolnikov, Phys. Rev. A **51**, R3433 (1995).

[8] K. S. Budil, P. Salières, A. L'Huillier, T. Ditmire, and M. D. Perry, Phys. Rev. A **48**, R3437 (1993).

[9] Y. Liang, M. V. Ammosov, and S. L. Chin, J. Phys. B **27**, 1269 (1994).

[10] L. V. Keldysh, Zh. Eksp. Teor. Fiz. **47**, 1945 (1964) [Sov. Phys. JETP **20**, 1307 (1965)].

[11] P. Dietrich, N. H. Burnett, M. Ivanov, and P. B. Corkum, Phys. Rev. A **50**, R3585 (1994).

[12] N. H. Burnett, C. Kan, and P. B. Corkum, Phys. Rev. A **51**, R3418 (1995).

[13] M. Möller, Y. Cheng, S. D. Khan, B. Zhao, K. Zhao, M. Chini, G. G. Paulus, and Z. Chang, Phys. Rev. A **86**, 011401 (2012).

[14] G. Sansone, L. Poletto, and M. Nisoli, Nature Phot. **5**, 655 (2011).

[15] T. Kanai, S. Minemoto, and H. Sakai, Phys. Rev. Lett. **98**, 053002 (2007).

[16] F. He, C. Ruiz, and A. Becker, Opt. Lett. **32**, 3224 (2007).

[17] H. Xu, H. Xiong, B. Zeng, W. Chu, Y. Fu, J. Yao, J. Chen, X. Liu, Y. Cheng, and Z. Xu, Opt. Lett. **35**, 472 (2010).

[18] C. Liu and M. Nisoli, Phys. Rev. A **85**, 013418 (2012).

[19] V. V. Strelkov, A. A. Gonoskov, I. A. Gonoskov, and M. Y. Ryabikin, Phys. Rev. Lett. **107**, 043902 (2011).

[20] V. V. Strelkov, M. A. Khokhlova, A. A. Gonoskov, I. A. Gonoskov, and M. Y. Ryabikin, Phys. Rev. A **86**, 013404 (2012).

[21] V. V. Strelkov, Phys. Rev. A **74**, 013405 (2006).

[22] D. Shafir, B. Fabre, J. Higuet, H. Soifer, M. Dagan, D. Descamps, E. Mével, S. Petit, H. J. Wörner, B. Pons, N. Dudovich, and Y. Mairesse, Phys. Rev. Lett. **108**, 203001 (2012).

[23] J. Higuet, H. Ruf, N. Thiré, R. Cireasa, E. Constant, E. Cormier, D. Descamps, E. Mével, S. Petit, B. Pons, Y. Mairesse, and B. Fabre, Phys. Rev. A **83**, 053401 (2011).

[24] A. D. Shiner, B. E. Schmidt, C. Trallero-Herrero, H. J. Wörner, S. Patchkovskii, P. B. Corkum, J. Kieffer, F. Légaré, and D. M. Villeneuve, Nature Phys. **7**, 464 (2011).

[25] T. Morishita, A.-T. Le, Z. Chen, and C. D. Lin, Phys. Rev. Lett. **100**, 013903 (2008).

[26] M. V. Frolov, N. L. Manakov, T. S. Sarantseva, M. Y. Emelin, M. Y. Ryabikin, and A. F. Starace, Phys. Rev. Lett. **102**, 243901 (2009).

[27] M. V. Frolov, N. L. Manakov, A. A. Silaev, N. V. Vvedenskii, and A. F. Starace, Phys. Rev. A **83**, 021405 (2011).

[28] J. Cooper and R. N. Zare, in *Lectures in Theoretical Physics*, Vol. XI-C, edited by S. Geltman, K. T. Mahanthappa, and W. E. Britten (Gordon and Breach, New York, 1969), pp. 317–337.

[29] M. V. Frolov, N. L. Manakov, and A. F. Starace, Phys. Rev. A **78**, 063418 (2008).

[30] N. L. Manakov, V. D. Ovsiannikov, and L. P. Rapoport, Phys. Rep. **141**, 319 (1986).

[31] L. D. Landau and E. M. Lifshitz, *Quantum Mechanics (Nonrelativistic Theory)* (Pergamon, Oxford, 1977).

[32] M. V. Frolov, A. V. Flegel, N. L. Manakov, and A. F. Starace, Phys. Rev. A **75**, 063408 (2007).

[33] M. V. Frolov, A. V. Flegel, N. L. Manakov, and A. F. Starace, Phys. Rev. A **75**, 063407 (2007).

[34] M. V. Frolov, N. L. Manakov, T. S. Sarantseva, and A. F. Starace, J. Phys. B **42**, 035601 (2009).

[35] M. V. Frolov, N. L. Manakov, T. S. Sarantseva, and A. F. Starace, Phys. Rev. A **83**, 043416 (2011).

[36] Note that since the TDER theory in Ref. [29] assumes there is only a single bound state having orbital angular momentum l, it thus takes into account only a single nonzero scattering phase $\delta_l(E)$. Consequently, the exact recombination amplitude in this case (owing to electric dipole selection rules) coincides with the Born-approximation result (cf. the discussion in Ref. [35]). However, we have proved for the more general two-state TDER model suggested in Ref. [35], in which two continuum electron channels have nonzero phases, that the exact photorecombination amplitude (not the Born approximation amplitude) enters the dipole moment (3). We emphasize that this technical detail having to do with the choice of TDER model does not affect the key result of this paper (i.e., whether or not the HHG yield for the case of elliptically polarized light may be factorized).

[37] R. Wong, *Asymptotic Approximations of Integrals* (SIAM, Philadelphia, 2001).

[38] B. M. Smirnov and M. I. Chibisov, Zh. Eksp. Teor. Fiz. **49**, 841 (1965) [Sov. Phys. JETP **22**, 585 (1966)].

[39] M. Lewenstein, Ph. Balcou, M. Yu. Ivanov, A. L'Huillier, and P. B. Corkum, Phys. Rev. A **49**, 2117 (1994).

[40] K. J. Schafer, B. Yang, L. F. DiMauro, and K. C. Kulander, Phys. Rev. Lett. **70**, 1599 (1993).

[41] P. B. Corkum, Phys. Rev. Lett. **71**, 1994 (1993).

[42] K. Blum, *Density Matrix Theory and Applications* (Springer, Berlin, 2012).

[43] A. D. DiChiara, E. Sistrunk, C. I. Blaga, U. B. Szafruga, P. Agostini, and L. F. DiMauro, Phys. Rev. Lett. **108**, 033002 (2012).

[44] T. Popmintchev *et al.*, Science **336**, 1287 (2012).

[45] M. Kutzner, V. Radojević, and H. P. Kelly, Phys. Rev. A **40**, 5052 (1989).

[46] S. Minemoto, T. Umegaki, Y. Oguchi, T. Morishita, A. T. Le, S. Watanabe, and H. Sakai, Phys. Rev. A **78**, 061402(R) (2008).

[47] H. J. Wörner, H. Niikura, J. B. Bertrand, P. B. Corkum, and D. M. Villeneuve, Phys. Rev. Lett. **102**, 103901 (2009).

[48] R. Kopold, W. Becker, M. Kleber, and G. G. Paulus, J. Phys. B **35**, 217 (2002).